Numerical Investigation on Bottom Gap of Micro Flow Sensor

Mohd Zulkiefly Abdullah[1], T. Kouta, Takuma Kamijo[2], Makoto Yamamoto[2], Shinji Honami[2] and Shouji Kamiunten[3]
1.School of Mechanical Engineering, Engineering Campus, Science University of Malaysia
14300 Nibong Tebal, Penang, Malaysia
Email: mezul@hotmail.com
2.Department of Mechanical Engineering, Tokyo University of Science
1-3 Kagurazaka, Shinjuku-ku, Tokyo 162-8601, Japan
Email: yamamoto@rs.kagu.tus.ac.jp
3.Yamatake Corporations
1-12-2, Kawana, Fujisawa, Kanagawa, 251-8522, Japan

Corresponding author ***M. Yamamoto*** *yamamoto@rs.kagu.tus.ac.jp*

ABSTRACT

The measurement of fluid flow is one of essential fields in sensor technology of process control. Important applications of a flow sensor can be found in mechanical engineering, medical equipment, semiconductor fabrication, automobile industry and so on. Especially, with the recent development of micro-machines, the flow measurement in micro-machines has been a critical issue. In many cases of micro-machines, however, the measurement must take place inside the channel or pipeline having a small cross-sectional area that usually inaccessible with the conventional sensors. Thus, the micro-scale sensor is needed for such purposes, and it must have excellent reliability under severe conditions and have to be realized at low cost. Recently, a great number of thermal flow sensors have been fabricated and employed with using MEMS technology. However, since the micro flow sensor is small in scale, it is too difficult to experimentally measure the flow field around such a sensor. Therefore, the use of CFD is necessary to understand the flow behaviour around the sensor, particularly near the sensor surface, before the improvement can be made.

In the present paper, in order to clarify the effect of bottom gap of a micro flow sensor, the 3D simulations have been performed, and the flow fields have been numerically investigated around the sensor for the two different installations; (Case A) the sensor is directly mounted on the channel wall surface and, (Case B) the sensor is installed at 0.5mm above the channel wall and supported by four square-sectioned pillars. Figures 1 and 2 illustrate the schematic diagram of the micro flow sensor. Using explicit MAC method, the incompressible governing equations were discretized by the 3rd-order upwind scheme proposed by Kawamura and Kuwahara (1984). Therefore, the present computation can be regarded as a quasi-direct numerical simulation (QDNS). Furthermore, the effects of Reynolds numbers on the flow field were also studied. The Reynolds numbers based on the sensor height and the maximum inflow velocity were varied from 700 to 7100, considering the practical application.

The typical results of velocity vectors in the symmetry plane are shown in Fig.3 at the Reynolds number of 7100. In Case A, the horseshoe vortex and the recirculation are growing and become more remarkable at the upstream and downstream of the micro flow sensor. The results also illustrate that the size increases with the Reynolds number (not shown here). On the other hand, in Case B, the velocity vector shows the flow is relatively smooth, and the horseshoe vortex and the recirculation are relatively smaller than those of Case A. This is caused from the small blockage of Case B sensor due to the bottom gap. These aspects would be preferable to the sensor performance. Fig.4 shows the boundary layer profiles at the center of micro sensor top surface for both cases. The profiles indicate that the boundary layer thickness is drastically reduced for the micro sensor installed with four pillars (Case B) at the higher Reynolds number. This is also desirable for the micro sensor.

The present results demonstrated that the bottom gap preferably changes the flow nature and the sensor performance would be improved, by installing the micro flow sensor with four pillars.

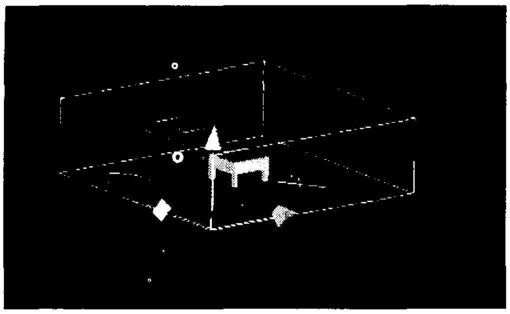

Fig.1 Model of Micro Flow Sensor with Bottom Gap

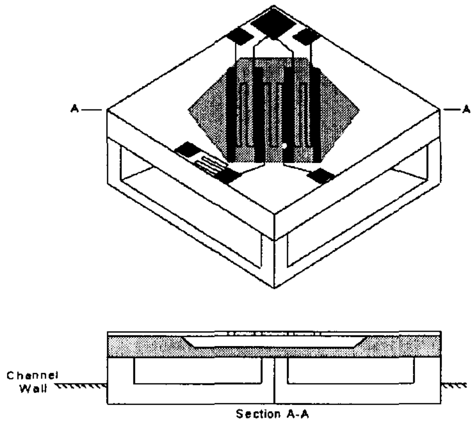

Fig.2 Schematic of Micro Flow Sensor

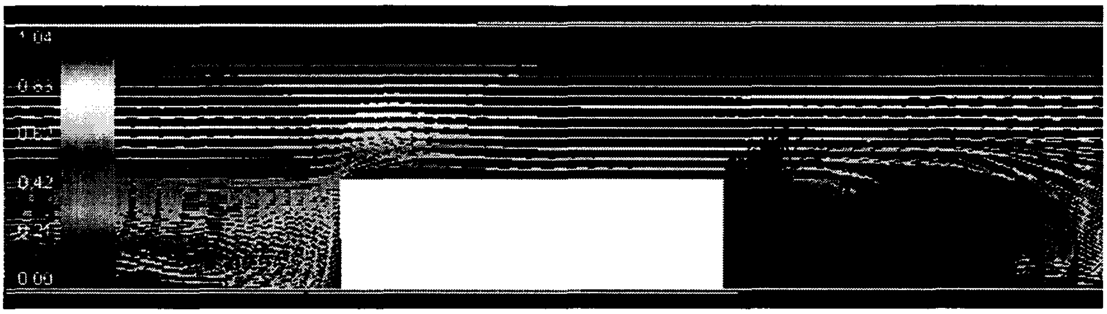

(a) without Bottom Gap (Case A)

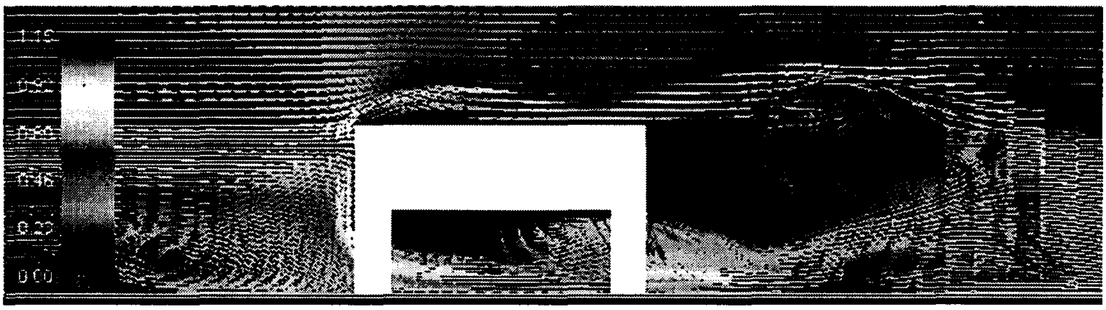

(b) with Bottom Gap (Case B)

Fig.3 Comparison of Velocity Vectors with and without Bottom Gap

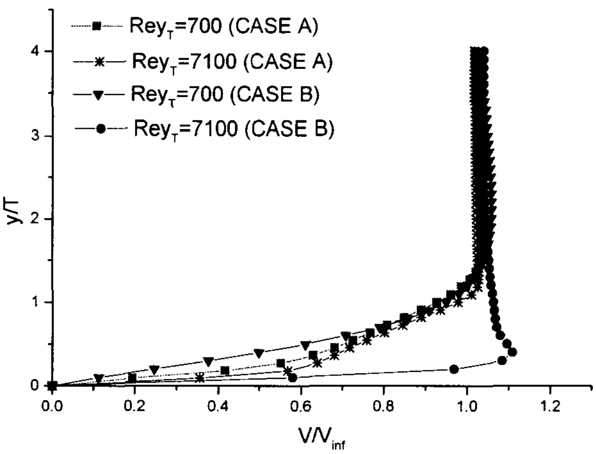

Fig.4 Boundary Layer Profile on Top Surface of Micro Flow Sensor